PROCEEDINGS OF SCIENCE

Precise decays rates for $\eta_c \to \gamma\gamma$ and $\eta_b \to \gamma\gamma$ from lattice QCD

Brian Colquhoun,[a,*] **Christine Davies**[a] **and G. Peter Lepage**[b]

[a] *SUPA, School of Physics and Astronomy, University of Glasgow, Glasgow, G12 8QQ, UK*
[b] *Laboratory of Elementary Particle Physics, Cornell University, Ithaca, New York, 14853, USA*
Street number, City, Country

E-mail: brian.colquhoun@glasgow.ac.uk, christine.davies@glasgow.ac.uk

The measurement of the decay rates $\eta_c \to \gamma\gamma$ and $\eta_b \to \gamma\gamma$ are part of the BES III and Belle II programmes respectively as tests of the Standard Model. Here we provide, for the first time, precise SM values for these decay rates using lattice QCD. For $\Gamma(\eta_c \to \gamma\gamma)$ we obtain 6.788(61) keV in good agreement with, but much more accurate than, experimental results using $\gamma\gamma \to \eta_c \to K\bar{K}\pi$. Our value is in 4 sigma tension with the PDG global fit result, however. Building on this study, we have been able to predict $\Gamma(\eta_b \to \gamma\gamma) = 0.526(30)$ keV. We also compare the ratio of the form factors to the meson decay constants with expectations from NRQCD to assess how well nonrelativistic effective theories work in these two cases.

42nd International Conference on High Energy Physics (ICHEP2024)
18-24 July 2024
Prague, Czech Republic

[*] Speaker

PoS(ICHEP2024)473

1. Introduction

In [1] we provided a clearer picture of the process $\eta_c \to \gamma\gamma$ through our lattice QCD calculation with a realistic sea, resulting in a sub-1% accuracy; a significant improvement over non-lattice methods. We have now performed a similar study of the process $\eta_b \to \gamma\gamma$, providing a prediction of the decay width that should be accessible to Belle II [2]. Calculations from theory have so far used nonrelativistic approaches where systematic uncertainties from relativistic and radiative corrections arise. Such uncertainties do not appear in our fully relativistic lattice calculation, but instead we deal with the statistical and systematic uncertainties from extrapolation to physical quark masses and the continuum limit.

2. Lattice calculation

Gluon field configurations used in these calculations were generated by the MILC collaboration [3, 4] and include the effects of $2+1+1$ flavours of quarks in the sea using the Highly Improved Staggered Quark (HISQ) formalism [5]. We also use the HISQ formalism for the valence quarks. Lattice spacings range from $a \approx 0.15$ fm down to $a \approx 0.06$ fm for the $\eta_c \to \gamma\gamma$ calculation, while for the $\eta_b \to \gamma\gamma$ process we use the range $a \approx 0.09$ fm to $a \approx 0.033$ fm to allow us to simulate at the physical b quark mass without the need for an additional extrapolation. Additionally, we perform analogous calculations for two intermediate meson masses using an appropriate selection of the available ensembles. We also include gauge ensembles that have light quarks tuned to their physical masses.

Our calculation proceeds by generating 3-point correlation functions between a temporal-axial vector current coupling to the η_h and two vector currents. We use the local currents $\gamma_x \otimes \gamma_x$ and $\gamma_z \otimes \gamma_z$ in spin-taste notation for the vector operators and $\gamma_5\gamma_t \otimes \gamma_x\gamma_y$ for the η_h. Momentum, $\omega_1 = M_{\eta_h}/2$, is inserted between the two vector operators in the y direction so that it is orthogonal to both vector current polarisations.

We take our 3-point correlator $C_{\mu\nu}$ and perform a weighted sum over time slices to set photon 1 on-shell [6–8], obtaining a 2-point correlator:

$$\tilde{C}_{\mu\nu} = a \sum_{t_{\gamma_1}} e^{-\omega_1 (t_{\gamma_1} - t_{\gamma_2})} C_{\mu\nu}(t_{\gamma_1}, t_{\gamma_2}, t_{\eta_c}). \tag{1}$$

We fit $\tilde{C}_{\mu\nu}$ to the form

$$\tilde{C}_{\mu\nu}(t_{\gamma_2}, t_{\eta_c}) = \sum_n a_n b_n f(E_n, t_{\gamma_2} - t_{\eta_c}); \quad f(E,t) = e^{-Et} + e^{-E(N_t - t)}. \tag{2}$$

Simultaneously, we fit to a standard 2-point correlator for the η_h:

$$C_{\eta_h}(t, t_{\eta_c}) = \sum_n a_n^2 f(E_n, t_{\gamma_2} - t_{\eta_c}) \tag{3}$$

and thus determine the ground-state contribution of the η_h to each of these correlators. The amplitude b_0 relates to the matrix element between the η_h and the two photons, and so the form factor is obtained by

$$\frac{F_{\mathrm{latt}(0,q_2^2)}}{a} = b_0 \sqrt{\frac{2}{aM_{\eta_h}} \frac{L_s}{\theta\pi}} Z_V^2, \tag{4}$$

where θ is the twist [9, 10] angle used to obtain the desired momentum with magnitude ω_1, and Z_V is the local vector renormalisation factor determined using the RI-SMOM intermediate scheme at 2 GeV [11, 12]. When $q_2^2 = 0$, this relates to the width for two on-shell photons by

$$\Gamma(\eta_h \to \gamma\gamma) = \pi\alpha_{\mathrm{em}}^2 Q_h^4 M_{\eta_h}^3 F(0,0)^2, \tag{5}$$

where Q_h is the electric charge of the heavy quark, and $1/\alpha_{\mathrm{em}}$ is taken as 137.036.

3. Results

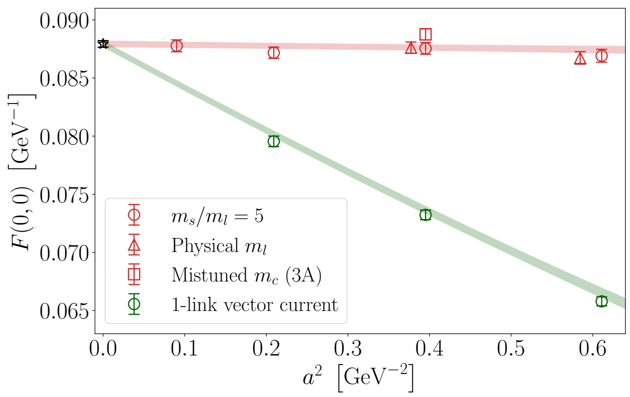

Figure 1: Fit for $F(0,0)$ from the process $\eta_c \to \gamma\gamma$. The red points and band show results using the current operators described in the text. The green points and band use an alternative set of operators that approach the same result in the continuum limit. Our final result comes from a simultaneous fit to both sets of data.

Our results for the form factor $F(0,0)$ from the $\eta_c \to \gamma\gamma$ process are shown in Fig. 1. The points are the lattice data and the bands come from a fit that is described in detail in [1]. The black star shows the continuum result at physical quark mass. We find

$$F(0,0) = 0.08793(29)_{\mathrm{fit}}(26)_{\mathrm{syst}}\ \mathrm{GeV}^{-1}; \quad \Gamma(\eta_c \to \gamma\gamma) = 6.788(45)_{\mathrm{fit}}(41)_{\mathrm{syst}}\ \mathrm{keV}, \tag{6}$$

where in each case the first error comes from the fit to the lattice data and the second accounts for additional systematic errors as described in [1].

A dimensionless ratio can also be constructed that has a straightforward limit in leading-order NRQCD:

$$R_{\eta_h} \equiv \frac{f_{hh}}{F_{\eta_h}(0,0)M_{hh}^2} = \frac{1}{2}\left(1 + O(\alpha_s) + O\left(v^2/c^2\right)\right), \tag{7}$$

where M_{hh} and f_{hh} are the mass and decay constant of a corresponding heavy-heavy meson respectively. We plot our results for this quantity for $\eta_c \to \gamma\gamma$ in Fig. 2 (left), where we chose the J/ψ as the appropriate hh meson in the ratio. The dotted line shows the leading-order NRQCD result and the black star depicts our physical result, $R_{\eta_c} = 0.4786(57)_{\mathrm{fit}}(14)_{\mathrm{syst}}$. The leading-order NRQCD approximation is better than might be expected, which is only revealed through an accurate lattice QCD calculation like this one.

Turning to the $\eta_b \to \gamma\gamma$ process, we performed a fit to the ratio R_{η_b}, the result of which is plotted in Fig 2 (right). A minor difference in this case is that we used decay constants and masses

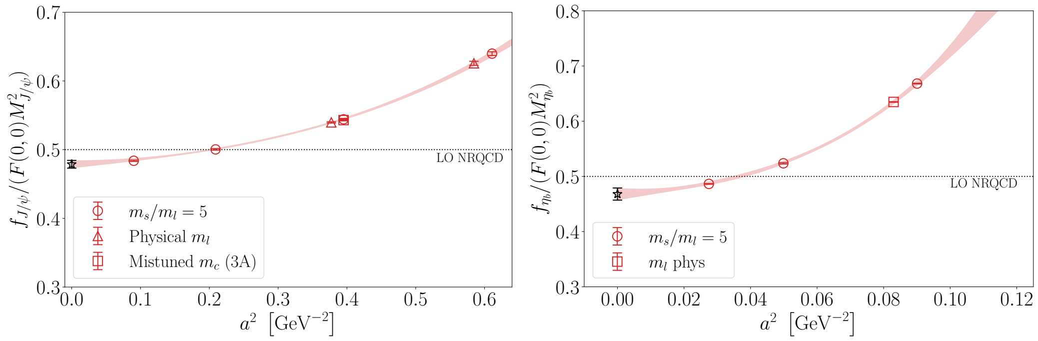

Figure 2: Fit results for the ratio R_{η_h} for the $\eta_c \to \gamma\gamma$ decays (left) and the $\eta_b \to \gamma\gamma$ decay (right). Black stars denote the results at physical light quark masses in the continuum.

for the pseudoscalar meson, η_b, rather than the vector, Υ, in this ratio since we could extract them conveniently from our correlator fits. We use three values of the lattice spacing and include one case where the light quarks are tuned to their physical value. The band shows our result at physical pion mass in the continuum. We find:

$$R_{\eta_b} = 0.468(11). \tag{8}$$

We isolate the form factor using $f_{\eta_b} = 0.724(12)$ MeV from lattice QCD [11] and the experimental η_b mass to determine

$$F(0,0) = 0.01751(50)\ \text{GeV}^{-1}. \tag{9}$$

We again convert to a decay width for this process, finding

$$\Gamma(\eta_b \to \gamma\gamma) = 0.526(30)_{\text{fit}}(1)_{\text{syst}}\ \text{keV}. \tag{10}$$

The systematic error accounts for missing QED effects and quark-line disconnected diagrams.

Figure 3 shows the mass dependence of the ratio R_{η_h}, where the intermediate points correspond to η_c masses of 4 GeV and 6.62 GeV. This dependence is very mild. The result at the charm mass has been recast so that the η_c decay constant and mass are used in the ratio – rather than the J/ψ values used in [1] – in order to compare appropriately with the other three points. The dash-dotted line shows the NRQCD expectation in the infinite mass limit. The dashed line shows the effect of adding in $O(\alpha_s)$ corrections to the NRQCD result, while the blue band depicts a relative ± 1 GeV$/M$ correction for missing $O(v^2/c^2)$ effects.

4. Discussion & Conclusions

Our calculation of the decay width $\Gamma(\eta_c \to \gamma\gamma)$ from lattice QCD, including – for the first time – the effect of u, d, s and c quarks in the sea has changed the theoretical picture of this process. Our result is in tension with the PDG fit result, which suffers from a poor χ^2 per degree of freedom, by over 4σ. We are in better agreement with the PDG average of those processes with η_c production from 2-photon fusion using the η_c decay mode to $K\bar{K}\pi$.

We provide a prediction of the decay width from the $\eta_b \to \gamma\gamma$ channel for the first time in lattice QCD and find $\Gamma(\eta_b \to \gamma\gamma) = 0.526(30)_{\text{fit}}(1)_{\text{syst}}$ keV. It is anticipated that this is within reach of

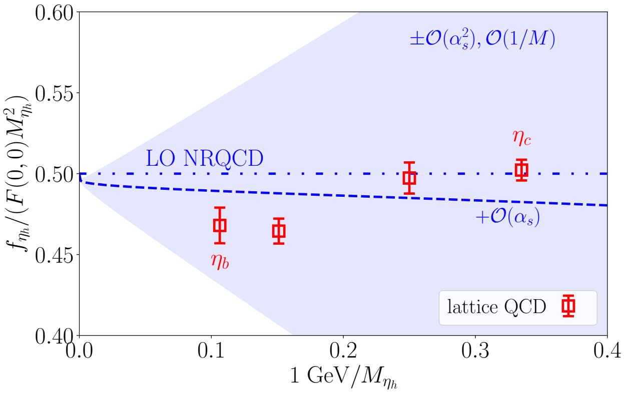

Figure 3: Results for R_{η_h} showing mild dependence of this ratio on the η_h mass. The blue lines and band denote expectations from NRQCD as described in the text.

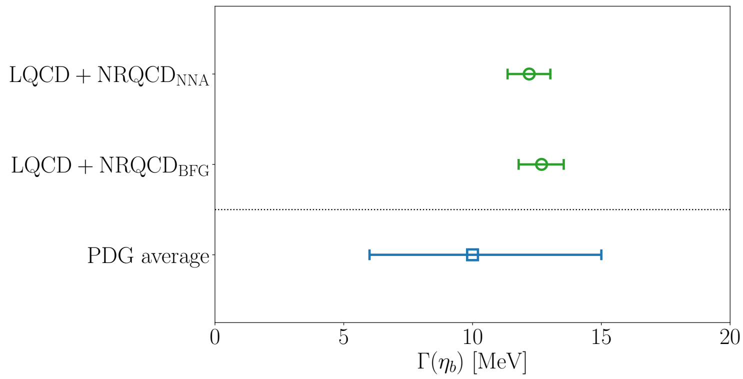

Figure 4: Inclusive width of the η_b. Green points combine our lattice results for $\Gamma(\eta_b \to \gamma\gamma)$ with pNRQCD calculations of the ratio $\Gamma(\eta_b)/\Gamma(\eta_b \to \gamma\gamma)$ from [13]. The blue point is the current PDG average [14].

Belle II. A determination of the inclusive width $\Gamma(\eta_b)$ is possible by combining our result with the ratio $\Gamma(\eta_b)/\Gamma(\eta_b \to \gamma\gamma)$ calculated using a potential NRQCD approach in [13]. We find $\Gamma(\eta_b \to \gamma\gamma) = 12.20(^{+42}_{-47})_{\mathrm{pNRQCD}}(70)_{\mathrm{LQCD}}$ MeV or $\Gamma(\eta_b \to \gamma\gamma) = 12.68(^{+47}_{-53})_{\mathrm{pNRQCD}}(72)_{\mathrm{LQCD}}$ MeV dependent on whether the value taken uses the NNA or BFG method in the potential NRQCD calculation. Both numbers are in good agreement with the current experimental average, but are a lot more accurate. We plot these values alongside the current experimental average taken from the PDG [14] in Fig. 4.

As an extension of this program of calculations, we are now studying the decay $J/\psi \to \gamma a$, where a is an axion-like particle (ALP). ALPs appear in theories beyond the Standard Model to explain, for example, the strong CP problem in QCD.

Acknowledgments

This work was performed using the Cambridge Service for Data Driven Discovery (CSD3), part of which is operated by the University of Cambridge Research Computing Service on behalf of the Science and Technology Facilities Council (STFC) DiRAC HPC Facility.

References

[1] HPQCD Collaboration , *Precise determination of decay rates for $\eta_c \to \gamma\gamma$, $J/\psi \to \gamma\eta_c$, and $J/\psi \to \eta_c$e+e- from lattice QCD*, Phys. Rev. D **108** (2023) 014513 [2305.06231].

[2] J.S. Lange and E. Prencipe, "Spectroscopy of bottomonium and its decays" at Hadron Spectroscopy: The Next Big Steps workshop at Mainz Institute for Theoretical Physics.

[3] MILC Collaboration , *Scaling studies of QCD with the dynamical HISQ action*, Phys. Rev. D **82** (2010) 074501 [1004.0342].

[4] MILC Collaboration , *Lattice QCD Ensembles with Four Flavors of Highly Improved Staggered Quarks*, Phys. Rev. D **87** (2013) 054505 [1212.4768].

[5] HPQCD & UKQCD Collaborations , *Highly improved staggered quarks on the lattice, with applications to charm physics*, Phys. Rev. D **75** (2007) 054502 [hep-lat/0610092].

[6] X.-d. Ji and C.-w. Jung, *Studying hadronic structure of the photon in lattice QCD*, Phys. Rev. Lett. **86** (2001) 208 [hep-lat/0101014].

[7] X.-d. Ji and C.-w. Jung, *Photon structure functions from quenched lattice QCD*, Phys. Rev. D **64** (2001) 034506 [hep-lat/0103007].

[8] J.J. Dudek, R.G. Edwards and D.G. Richards, *Radiative transitions in charmonium from lattice QCD*, Phys. Rev. D **73** (2006) 074507 [hep-ph/0601137].

[9] C.T. Sachrajda and G. Villadoro, *Twisted boundary conditions in lattice simulations*, Phys. Lett. B **609** (2005) 73 [hep-lat/0411033].

[10] D. Guadagnoli, F. Mescia and S. Simula, *Lattice study of semileptonic form-factors with twisted boundary conditions*, Phys. Rev. D **73** (2006) 114504 [hep-lat/0512020].

[11] D. Hatton, C.T.H. Davies, J. Koponen, G.P. Lepage and A.T. Lytle, *Bottomonium precision tests from full lattice QCD: Hyperfine splitting, Υ leptonic width, and b quark contribution to $e^+e^- \to$ hadrons*, Phys. Rev. D **103** (2021) 054512 [2101.08103].

[12] HPQCD Collaboration , *Renormalizing vector currents in lattice QCD using momentum-subtraction schemes*, Phys. Rev. D **100** (2019) 114513 [1909.00756].

[13] N. Brambilla, H.S. Chung and J. Komijani, *Inclusive decays of η_c and η_b at NNLO with large n_f resummation*, Phys. Rev. D **98** (2018) 114020 [1810.02586].

[14] Particle Data Group , *Review of particle physics*, Phys. Rev. D **110** (2024) 030001.